RSC Advances

PAPER

View Article Online
View Journal | View Issue

Cite this: *RSC Adv.*, 2021, **11**, 34699

Construction and properties of the antibacterial epitaxial transition layer on a zirconia ceramic surface

Xiuju Liu,[a] Qiuli Cheng,[b] Yanlin Zhu,[c] Shiyang Yu,[a] Yanyan Hou,[a] Zhanchen Cui*[b] and Song Zhu*[a]

Received 28th August 2021
Accepted 19th October 2021

DOI: 10.1039/d1ra06496g

rsc.li/rsc-advances

Secondary caries is one of the main causes of dental zirconia restoration failure in the clinic. Therefore, it is urgent to improve the antibacterial performance of zirconia ceramics to reduce the occurrence of secondary caries. In this study, a quaternary ammonium compound antibacterial polymer was innovatively synthesized by solution polymerization with a quaternary ammonium salt monomer as the antibacterial component. The antibacterial epitaxial transition layer was successfully prepared on the surface of zirconia ceramics by the hydroxyl group on HEMA reacting with the siloxane group in the KH570 hydrolysate, which makes the antibacterial polymer indirectly chemically combine with the silicate epitaxial transition layer. The antibacterial epitaxial transition layer exhibited excellent mechanical properties, satisfactory biocompatibility and significant antibacterial effects, and the maximum antibacterial rate is 99%. The antibacterial epitaxial transition layer plays an important role in preventing secondary caries and improving the success rate of clinical zirconia ceramic restorations.

1 Introduction

Because of the excellent biocompatibility, good aesthetic characteristics, high fracture toughness and mechanical strength produced by the phase transformation toughening mechanism, zirconia ceramics have become a hot topic in oral materials science. However, one of the main reasons for clinical failure of zirconia restoration is secondary caries.[1] Secondary caries is defined as "lesions at the edge of existing restorations".[2] Secondary and primary caries exhibit no differences in etiology. They are all chronic infectious diseases caused by bacteria. When a crack occurs between the prosthesis and the tooth tissue, and saliva enters the crack, bacteria adhering to saliva invade the entire crack. When nutrients and time are sufficient, bacteria propagate and produce acid, which leads to demineralization of the tooth tissue and formation of secondary caries. Due to the differences in the thermal expansion coefficient of zirconia ceramics, tooth tissue and adhesive, cold and hot stimulation changes in the oral environment will cause microcracks at the edge of the restoration, which will result in bacterial invasion and secondary caries. Bacteria and plaque biofilms are essential factors for secondary caries.[3,4] Therefore, improving the antibacterial properties of zirconia ceramic restorations, inhibiting the invasion of bacteria, killing bacteria at the edge of cracks, and sealing edges are important measures to prevent secondary caries.

The simplest way to endow restorative materials with antibacterial properties is to add widely recognized antibacterial agents, including nano silver, chlorhexidine, quaternary ammonium salt, triclosan, chitosan, antibiotics, *etc.* At present, the main antibacterial agents are soluble and polymerizable antibacterial agents. The soluble antibacterial agent is dispersed in the material by physical dissolution, and produces antibacterial effects by continuous exusion. This method is simple and easy to operate, but it is easy to produce a "sudden release effect" due to its failure to control the release kinetics, which can not guarantee the long-term antibacterial effect. In addition, the continuous separation of antibacterial components makes the material appear to have a void structure, which destroys the integrity of the bonding interface and the durability of the bonding effect, and reduces the mechanical properties of the material.[5] In the 1990s, Imazato *et al.*[6] introduced the concept of a "polymerizable antibacterial agent" into the field of dental materials. "Polymerizable antibacterial agent" refers to an antibacterial agent that has the function of polymerization. Based on chemical methods, the antibacterial functional groups are firmly combined with the polymer chain of the resin matrix, and the contact antibacterial effect is stable and independent of the release of antibacterial active ingredients. These agents exhibit great advantages and good application prospects to achieve stable and long-term antibacterial modification of

[a]*Department of Prosthetic Dentistry, School and Hospital of Stomatology, Jilin University, Changchun 130021, P. R. China. E-mail: zhusong1965@163.com*

[b]*State Key Lab of Supramolecular Structure and Materials, College of Chemistry, Jilin University, Changchun 130021, P. R. China*

[c]*Department of Dental Implantology, School and Hospital of Stomatology, Jilin University, Changchun, P. R. China*

resin materials and overcome the adverse effects of traditional soluble antibacterial agents on the mechanical properties and aesthetic properties of the materials.[7]

Quaternary ammonium compounds (QACs) are broad-spectrum antibacterial agents of cationic surfactants. The materials containing these antibacterial agents exhibit a long-lasting antibacterial effect when in contact with bacteria, and do not release antibacterial components. The antibacterial properties and biocompatibility of QACs are closely related to their chemical structures. Studies show that within a certain range, the antibacterial activity of QACs increases with the length of the hydrophobic alkyl chain on the nitrogen atom,[8,9] and excessive hydrophobicity often prevents membrane penetration and increases cytotoxicity.[10] Following the theory of a "polymerizable antibacterial agent", some scholars combined quaternary ammonium group with methacryloyl group for the first time in 1994, and successfully developed a QACs antibacterial monomer that can polymerize with a traditional methacryloyl monomer, namely: methacryloyloxydecyl pyridinium bromide (MDPB).[11] Subsequently, a series of QACs antibacterial agents have been synthesized, which have long-term and lasting antibacterial effects and prevent the occurrence of secondary caries.[12–14]

QACs are a general term for a class of compounds that has been widely studied due their relatively low toxicity and broad antibacterial spectrum. Compared with other antibacterial agents, QACs have the advantages of good biocompatibility and long-lasting biological effects, and are often used in the surface disinfection of medical devices, skin and mucous membrane disinfection and oral cleaning.[15–17] In recent years, QACs have been widely used in the antibacterial modification of oral restorative materials.[18–25]

In recent years, some scholars have added QACs to composites such as resin, adhesive system, acrylic resin and dental pulp materials.[26,27] However, the application of QACs are not limited to these. Several studies had incorporated QACs into bone cements, titanium implants, pulp capping materials, cavity disinfectant, resin cement, *etc.*[7,18,23,24] These studies have shown that QACs possess antimicrobial activities against bacteria and fungi including *S. mutans*, *L. acidophilus*, *C. albicans*, *E. faecalis* which could decrease the occurrence of secondary caries. The application of QACs in dental materials is very promising. QACs have been also proved has good biocompatibility and do not represent a threat to human health.

In previous work, we successfully constructed a silicon epitaxial transition layer on the surface of zirconia ceramics, which improved the shear bond strength and aging resistance of zirconia ceramic restorations, and exhibited good biological safety.[26] To effectively prolong the service life of zirconia ceramic restorations and reduce the incidence of secondary caries, a quaternary ammonium salt antibacterial polymer was designed and synthesized in this study. The antibacterial polymer was chemically combined with the silane coupling agent KH570 by using –OH groups on HEMA. The shear bond strength of the zirconia ceramic restoration was improved, and its antibacterial property was effective. The antibacterial polymer was added into the 3 wt% epitaxial transition layer at the mass fractions of 0 wt% (control group), 1 wt%, 3 wt%, 5 wt% and 7 wt%, and its antibacterial effect and biocompatibility were evaluated. Fig. 1 presents the design and flow chart of this experiment.

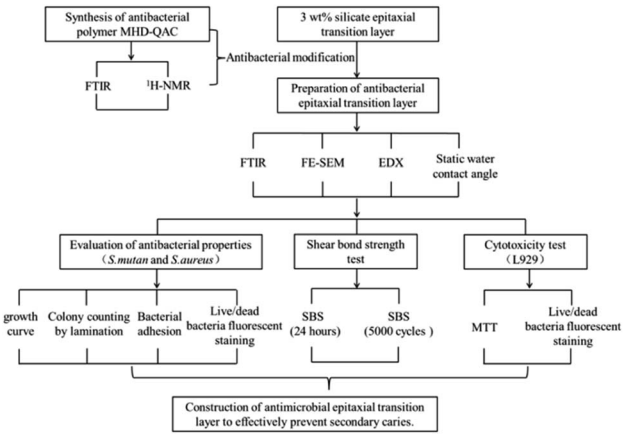

Fig. 1 Experimental design.

2 Materials and methods

2.1 Synthesis of quaternary ammonium salt antibacterial polymer

The polymers are synthesized by simple radical solution polymerization. Methyl methacrylate (MMA, Alfa Aesar Sigma Company, USA) (50 mmol, 5.006 g), hydroxyethyl methacrylate (HEMA, Sigma Company, USA) (20 mmol, 2.603 g) and dimethylaminoethyl methacrylate (DMA, Sigma Company, USA) (30 mmol, 4.716 g) were mixed in a 250 ml flask, tetrahydrofuran (THF, Sigma company, USA) (100 ml) was added, and the mixture was heated at 70 °C. After nitrogen degassing for 30 minutes, azobisisobutyronitrile (AIBN, Sigma Company, USA) (1 mmol, 0.164 g) was added into the mixture as an initiator. The polymerization was performed at 70 °C for 12 hours. The reaction mixture was purified in petroleum ether, and the unreacted monomers (MMA, DMA and HEMA) were removed. After vacuum drying, the polymer MMA-HEMA-DMA was obtained, which was labeled MHD. MHD (1.232 g) was dissolved with excess bromododecane (Alfa Aesar, USA) (0.374 g) in a 50 ml flask containing 15 ml nitrile and reacted at 80 °C for 24 hours. Then, the product was dissolved in chloroform, precipitated in hexane and purified. The polymer MHD-QAC was obtained after drying at 45 °C in a vacuum oven for 24 hours. ^{1}H NMR spectra were analyzed by a Bruker-AVANCE nuclear magnetic resonance spectrometer (AVANCEIII500, Switzerland), and Fourier transform infrared (FT-IR) spectra were recorded with a Fourier transform infrared spectrometer (VERTEX 80V; Bruker, Germany).

2.2 Construction of the antibacterial epitaxial transition layer on zirconia ceramic surface

2.2.1 Preparation of a 3 wt% silicate epitaxial transition layer and hydrolysis of the silane coupling agent KH570 (ref.

28). Using 90 wt% ethylene glycol ether and 10 wt% deionized water as diluents, the original 20 wt% silicate solution (1.5 g), diluent (6.5 g), 1‰ levelling agent (1.0 g) and 10% ethylene glycol (1.0 g) were prepared into a silicate solution with a concentration of 3 wt%. The sintered $8 \times 8 \times 3$ mm^3 zirconia ceramic block (LAVA, 3M ESPE, USA) were polished with 600-, 800-, 1000- and 1500-grit silicon carbide abrasive papers for 10 s under running water, cleansed ultrasonically for 10 min in 70% ethanol and rinsed with 70% ethanol using an ultrasonic bath (Eurosonic Energy, Euronda Inc., Vicenza, Italy). They were then air-dried at room temperature for 30 min. The zirconia ceramic block was sandblasted for 10 seconds at a distance of 10 mm from the bonding surface with 50 μm Al_2O_3 particles at 0.25 MPa pressure. After sandblasting, zirconia specimens were immersed in silicate solution of 3 wt%, soaked for 5 minutes under ultrasonic vibration conditions, and then removed. After standing at room temperature for 24 hours, the specimens were heated at 50 °C for 10 hours. After the 3 wt% silicate epitaxial transition layer specimens cooled to room temperature, they were rinsed with deionized water to remove the unreacted solution and then dried in air.

The hydrolysate consisting of ethyl orthosilicate (6.0 g), anhydrous ethanol (30.0 g), glacial acetic acid (0.1 g) and deionized water (0.3 g) was stirred by magnetic force for 1 hour. The silane coupling agent γ-methacryloxypropyltrimethoxysilane (KH570) (3.0 g) with a C=C group was dropped into the above mixed solution, and the solution was sufficiently hydrolyzed by magnetic stirring for 24 hours to prepare the KH570 hydrolysate.

2.2.2 Preparation of the MHD-QAC antibacterial epitaxial transition layer. MHD-QAC was added to the KH570 hydrolysate in different mass fractions (0 wt%, 1 wt%, 3 wt%, 5 wt%, 7 wt%). Zirconia ceramic specimens with a 3 wt% silicate epitaxial transition layer were placed into the above KH570 hydrolysate containing different concentrations of MHD-QAC. After 10 hours, the specimens were removed and heated at 50 °C for 3 hours to prepare the MHD-QAC antibacterial epitaxial transition layer.

2.3 Surface characterization

The zirconia modified by the MHD-QAC antibacterial epitaxial transition layer was analyzed by a Fourier transform infrared (FT-IR) spectrometer (VERTEX 80V; Bruker, Germany). The surface morphologies of all samples were examined by scanning electron microscopy (SEM, S-4800, Hitachi, Japan). The elemental compositions of the samples were analyzed by energy-dispersive X-ray spectroscopy (EDX, QUANTAX 400, Luke AXS Co., Ltd., Germany). The static water contact angle was determined by a droplet imaging analysis system (DSA20, MK2 KR SS Edward Keller Company, Germany) by the hanging drop method using deionized water on the surface of the samples at different positions.

2.4 Antibacterial activity test

2.4.1 Culture of experimental strains. Frozen *Streptococcus mutans* (*S. mutans*, ATCC35668, American Strain Preservation Center) was resuscitated and inoculated in BHI agar medium (Beijing Solarbio Technology Co., Ltd., China) and cultured in an anaerobic environment for 48 hours. The strain was identified as pure culture by morphological and biochemical tests and then passed to the third generation. A single colony was selected using an inoculation ring and inoculated in BHI liquid culture medium. After 48 hours of anaerobic culture, a 1×10^9 CFU L^{-1} bacterial suspension was prepared.

2.4.2 Bacterial growth curve. The specimens were placed in a sterile plate, transferred to an ultraclean bench (BLB-1300, Suzhou Sujing Baishen Technology Co., Ltd.), subjected to UV irradiation for 2 hours and then turned over after 1 hour.

The sterilized specimens were placed in sterile centrifuge tubes containing 4 ml bacterial suspension (1×10^9 CFU L^{-1}) and then incubated in a bacteria incubator (SLI-1200, SANYO, Japan) for 48 hours at a relative humidity of greater than 90% and a temperature of 37 °C. The co-culture specimen was removed, and the specimen was gently washed with PBS buffer to remove non-adherent bacteria. The specimens were then replaced in a centrifuge tube containing fresh liquid BHI medium and cultured for 2 hours, 4 hours, 6 hours, 8 hours, 10 hours, 12 hours and 24 hours. The co-cultured centrifuge tube was ultrasonically vibrated for 10 minutes so that the bacteria adhering to the specimen were shaken down. Then, the absorbance value (OD) of co-culture bacterial suspensions was measured using a microplate reader (BL340, Biotech, USA) at 600 nm. The above experiment was repeated three times.

2.4.3 Colony counting by film test. Approximately 50 μl bacterial suspension (1×10^9 CFU L^{-1}) was dispersed onto the surface of each sterile specimen, which was then covered with a sterile polyethylene film. After incubation in a bacterial incubator for 48 hours at a relative humidity greater than 90% and temperature of 37 °C, the specimens were thoroughly washed with 10 ml PBS buffer 10 times. The eluent was diluted 10^3 times by gradient and 50 μl was evenly coated on BHI agar medium plate, and cultured in anaerobic environment at 37 °C for 48 hours. Finally, the viable colony (CFU per sample) was counted. The antibacterial rate was calculated using the following formula:

$$R(\%) = \frac{B - A}{B} \times 100$$

where R is the antibacterial rate; A is the colony number of the experimental specimens; and B is the colony number of the control group.

Referring to the national HG/T 3950-2007 about antibacterial coating antibacterial standard, the antibacterial effect was

Table 1 Antibacterial classification

Antibacterial rate	Antibacterial grade	Antibacterial effect
≥99	I	Strong antibacterial
90–99	II	Antibacterial
<90	0	No antibacterial

graded (Table 1). The experimental results must meet the following two conditions: (1) the above experimental operation was repeated three times, and the average value was taken after statistical analysis; and (2) the number of viable colonies of three parallel specimens in the same group should equal the in accordance with: maximum value − minimum value/average value ≤ 0.3.

2.5 Antibacterial adhesion test

(1) Bacterial adhesion plate colony count

The sterilized specimens were placed into tubes containing 2 ml bacterial suspension (1×10^9 CFU L^{-1}) and cultured in an anaerobic environment for 48 hours. The specimens were removed and rinsed with sterile PBS buffer for 10 seconds to remove the non-adherent bacteria from the surface. The adherent bacteria were detached ultrasonically from the specimens in 10 ml PBS buffer for 5 minutes. The washing solution was diluted 10^2 times by gradient and 50 μl was evenly coated on BHI agar medium plates. After 48 hours of anaerobic culture, the colonies were counted.

(2) FE-SEM observation of the adherent bacteria

The sterilized specimens were placed in 24-well plates, and a 2 ml bacterial suspension (1×10^9 CFU L^{-1}) was added to each well. After co-cultured in an anaerobic environment for 48 hours, the specimens were removed and washed gently with sterile PBS buffer to remove the non-adherent bacteria. Then, the co-cultured specimens were sequentially placed in 2.5% glutaraldehyde (Sigma, USA) for 8 hours at 4 °C. Next, the specimens were placed in 30%, 50%, 70%, 80%, 90%, 100% and 100% ethanol solutions for gradient dehydration, with incubation in each solution lasting 15 minutes. The specimens were dried by a vacuum dryer at a critical point of CO_2 and sprayed with gold coating. Finally, FE-SEM was used to observe the morphology of adherent bacteria on the surface of the specimen.

2.6 Live/dead bacteria fluorescent staining

The sterilized specimens were placed in a 24-well plate, and 2 ml bacterial suspension (1×10^9 CFU L^{-1}) was added to each well. After culture for 48 hours in an anaerobic environment, the specimens were removed, gently washed with sterile PBS buffer to remove the floating bacteria on the surface of the specimens, and then moved to a new 24-well plate. The LIVE/DEAD BacLight Bacterial Viability Kit (Thermo Science Fisher, United States) was added to the surface of specimens of each group evenly, and the plate was incubated at room temperature for 15 minutes in the darkroom. The specimens were placed under a fluorescence microscope (Olympus, Japan), and the bacteria were observed by dual-channel scanning. The green channel (excitation wavelength 488 nm, green luminescence) was used to observe the living bacteria with intact cell membrane (stained with SYTO9 to emit green fluorescence). The red channel (excitation wavelength 543 nm, red luminescence) was used to observe the dead bacteria with damaged cell membranes (stained with propidium iodide to show red fluorescence).

The culture environment and culture time described in these antimicrobial experiments were for *S. mutan*. In the same steps as described above, the bacteria were replaced with *Staphylococcus aureus* (*S. aureus*, ATCC25922, Strain Preservation Center of the United States), and the medium, culture cycle and culture conditions were replaced with LB medium (Beijing Solarbio Technology Co., Ltd., China), 24 hours and an aerobic environment, respectively.

2.7 Shear bond strength test

2.7.1 Luting. Resin cement Multilink Speed (Ivoclar Vivadent AG, Liechtenstein) was activated according to the instructions provided by the manufacturer. A light-cured composite resin cylinder Filtek Z350 (3M ESPE, USA) (diameter 2.7 mm, height 4.0 mm) was placed onto the zirconia surface (prepared in 2). The excess cement was removed after light polymerization for 3–5 seconds using a light curing machine (SLC-VIIIA, Hangzhou Quartet Medical Devices Co., Ltd., Hangzhou, China) with a light power density of 900 mW cm^{-2} monitored by a Cure Rite radiometer. The specimens were light polymerized from two opposite lateral directions of the block for 20 seconds each. The bonded specimens were stored in distilled water at 37 °C for 24 hours. Then, each group was divided into two subgroups: the first subgroup ($n = 9$) was assessed for the bond strength; and the second subgroup ($n = 9$) was subjected to thermal cycling (Proto-Tech, Micoforce, Portland, OR, USA) for 5000 cycles between 5.0 ± 0.5 °C and 55.0 ± 0.5 °C prior to bond strength testing. The dwell time in each deionized water bath was 30 seconds.

2.8 Shear bond strength

The shear bond strength (SBS) was measured with a universal testing machine (AG-Xplus10 KN; Shimadzu, Kyoto, Japan). A constant load of 1 kN was applied with a cross-head speed of 1.0 mm min^{-1} until failure occurred. The SBS was calculated according to the following formula: $P = F/S$, where P is the SBS (MPa), F is the maximum shear force (N), and S is the bonding area (mm^2).

2.9 Cytotoxicity test *in vitro*

2.9.1 MTT test. The sterilized specimens were placed into sterile plates. Then, sterile cell high-glucose medium (Nanjing Jiancheng Biological Co., Ltd., China) was added at a ratio of 10 ml : 1 cm^2, and the plates were placed in a CO_2 incubator (MCO-20IL, Sanyo, Japan) at 37 °C for 72 hours to prepare the extraction solution.

Mouse fibroblast L929 (L929, Cells Resource Center, Shanghai Institutes of Biological Science, China) cell suspension in logarithmic growth phase at a concentration of 2×10^4 ml^{-1} was added into a 96-well plate (Costa, USA) with 2000 cells per well. The following eight groups were then used for subsequent experiments: blank control (pure high glucose medium), negative control (PE), positive control (phenol), 0 wt% group, 1 wt% group, 3 wt% group, 5 wt% group and 7 wt% group. The marked 96-well plates were placed in a cell incubator (5% CO_2, 95% humidity). After incubation for 24 hours at 37 °C, the

Table 2 Classification of cytotoxicity

RGR	Toxicity grade	Safety standards
≥100	0	Safe
75–99	I	Safe
50–74	II	Insecurity
25–49	III	Insecurity
1–24	IV	Insecurity
<1	V	Insecurity

supernatant was removed, and 100 μl extraction solution was added into each well. After culture for 24, 48 and 72 hours, the cell culture was terminated, and the cell culture medium in the pore plate was extracted and washed gently with PBS. Next, 20 μl MTT solution was added to each well and incubated for 4 hours. The MTT-containing medium was then removed and replaced by 150 μl dimethyl sulfoxide. The absorbance (A) was measured at 490 nm with a microplate reader (BL340, Biotech, USA). The relative growth rate (RGR) of the cells was calculated using the following formula: RGR = $A_{\text{experimental group}}/A_{\text{blank control group}} \times 100\%$. According to the relationship between the relative growth rate and cytotoxicity classification (Table 2),[29] the toxicity grade and safety standard of the specimen were judged.

2.10 Calcein-AM and PI live/dead cell staining

The logarithmic growth phase of L929 cells at a concentration of 5×10^4 ml^{-1} was added to 6-well plates at 2 ml per well. After culturing for 24–48 hours at 37 °C and 5% CO_2, the supernatant of the experimental group was replaced by the material extract, while the blank control group was replaced by fresh medium, and co-cultured for 24 hours. Then, the liquid in the orifice plate was discarded, and the plate was rinsed gently with sterile PBS buffer. Calcein-AM and PI dye solution were added to the 6-well plates at 1 ml per well. After incubation for 15 minutes, the cells were observed and recorded using an inverted fluorescence microscope (Olympus, Japan). Finally, the proportion of living cells was calculated.

2.11 Statistical analysis

The statistical analyses were performed using Statistical Package for the Social Sciences (SPSS) statistical software (SPSS version 22.0, SPSS Inc., Chicago, IL, USA). After testing for normality and homoscedasticity using the Kolmogorov–Smirnov test, ANOVA was used to test the significance of the experimental data.

3 Results and discussion

3.1 Synthesis and characterization of MHD-QAC

Fig. 2 shows the synthetic routes of the antibacterial copolymer MHD-QAC. Fig. 3 shows the FT-IR (A) and ^{1}H NMR spectra (B) of MHD-QAC. As presented in Fig. 3A, the absorption peak at 3420 cm^{-1} is the characteristic stretching vibration peak of the hydroxyl group, and 2950 cm^{-1} is the stretching vibration peak of the methyl group. As shown in Fig. 3B, the proton resonance

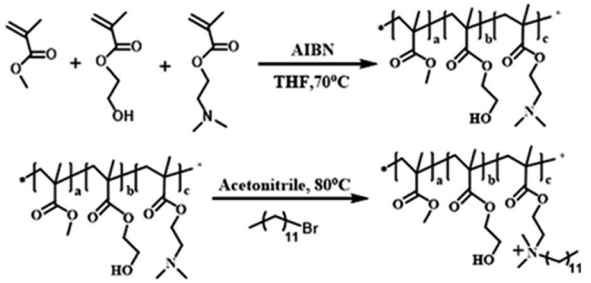

Fig. 2 Synthesis routes of MHD-QAC.

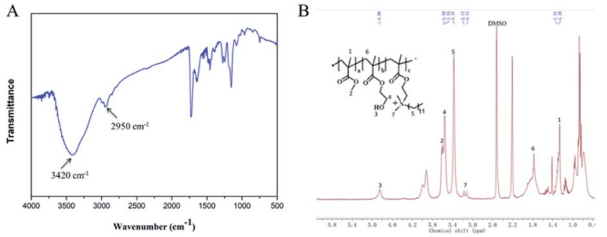

Fig. 3 FT-IR (A) and ^{1}H NMR (B) spectra of MHD-QAC.

at 3.37 ppm is from the methyl group of bromododecane, that at 3.58 ppm is from the methyl group of MMA and that at 4.86 ppm is from hydroxyl hydrogen atom of HEMA. In conclusion, the FT-IR and ^{1}H NMR results indicated that the MHD-QAC copolymer was innovatively designed and synthesized.

The MHD-QAC polymers are synthesized by simple radical solution polymerization. In the preliminary exploration stage, we tried different molar ratios of M : H : D. The properties of polymers with different M : H : D molar ratios, such as glass transition temperature, are different. When the M : H : D molar ratio is 50 : 20 : 30, the polymers have certain thermal stability. DMA is a monomer with antibacterial properties after quaternization. There are hydroxyl groups in HEMA that can react to KH570. So, we choose to copolymerize DMA with MMA and HEMA in order to combine the antibacterial polymer with the surface of zirconia ceramics in the form of chemical bond.

3.2 Characterization of the antibacterial epitaxial transition layer

3.2.1 FT-IR spectroscopy. Fig. 4 shows the FT-IR spectra of the antimicrobial epitaxial transition layer. In the FT-IR spectra of 1 wt%, 3 wt%, 5 wt% and 7 wt%, the obvious absorption peak of the carbonyl C=O bond in MMA is observed at 1720 cm^{-1}, and the obvious absorption peak of the amino N–H bond is observed at 2937 cm^{-1}. Therefore, an antimicrobial epitaxial transition layer containing MHD-QAC was successfully prepared on the zirconia surface. MHD-QAC was mixed with KH570 hydrolysate to act on the silicate epitaxial transition layer. In the blend system, the hydroxyl group on HEMA reacts with the siloxane group in the KH570 hydrolysate, which makes the antibacterial polymer indirectly combine with the silicate epitaxial transition layer.

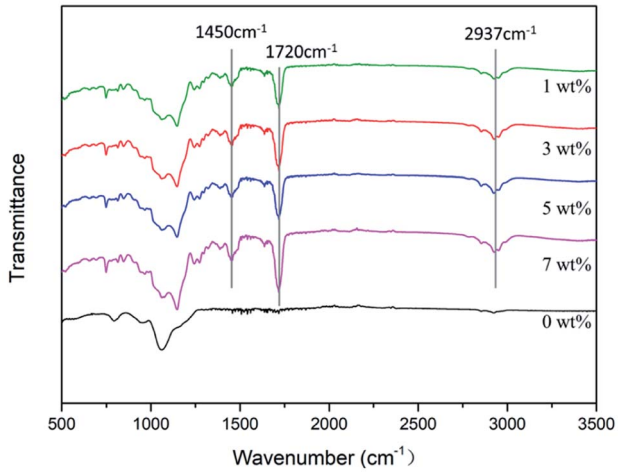

Fig. 4 FT-IR spectra of zirconia surfaces.

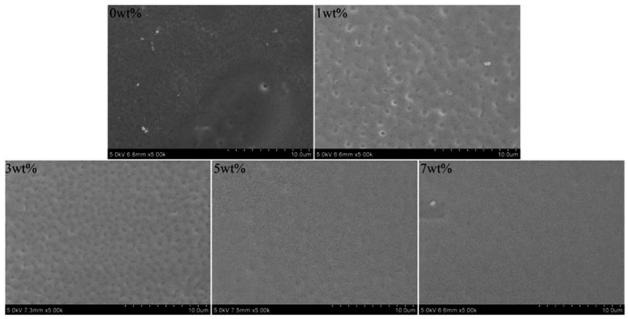

Fig. 5 SEM results of zirconia surfaces (×5000).

3.2.2 FE-SEM analysis. Fig. 5 presents the SEM images of the antibacterial epitaxial transition layer on the zirconia surface. A uniform and dense coating is observed on the surface of each sample, without cracks. In particular, the coatings of the 1 wt% and 3 wt% specimens exhibit a slightly concave structure, while those of the 5 wt% and 7 wt% specimen coatings are relatively dense, smooth and flat.

3.2.3 EDX analysis. Fig. 6 shows the EDX results of the antibacterial epitaxial transition layer. Only C, O and Si are present on the surface of the 0 wt% group, whereas N appears

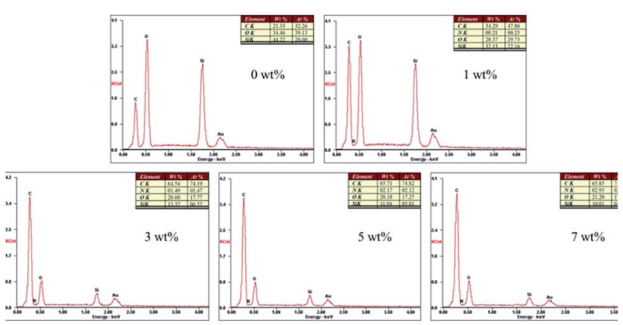

Fig. 6 EDX spectra and elemental composition of the zirconia surfaces.

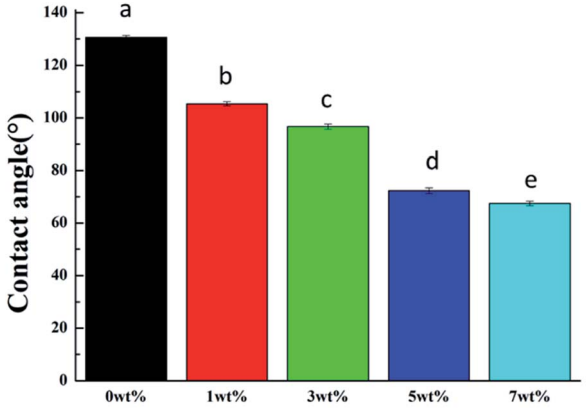

Fig. 7 Water contact angle of zirconia surfaces. Different letters indicate statistical differences ($P < 0.05$).

on the surface of the 1–5 wt% groups. In addition, the content of N increases with increasing MHD-QAC content.

3.2.4 Contact angle. Fig. 7 presents the surface water contact angle of the antibacterial epitaxial transition layer. Compared with that of the control group, the contact angle of water on the surface of the 1–7 wt% groups decreased significantly ($P < 0.01$). Because MHD-QAC is a hydrophilic polymer and contains cations, the surface contact angle of the epitaxial transition layer decreases and hydrophilicity increases after adding antibacterial polymer, which is conducive to the infiltration of adhesive.

3.3 Antibacterial activity

Numerous methods are available to evaluate the antibacterial properties of materials. At present, the generation of bacterial growth curves, colony counting by film tests, bacterial adhesion and live/dead bacteria fluorescent staining are the most commonly used experimental methods.[30] *S. mutans* and *S. aureus* were selected as experimental strains to evaluate the antibacterial properties of the antibacterial epitaxial transition layer on the surface of zirconia ceramics based on the above four methods. Streptococcus mutans is the main cariogenic bacterium.[31,32] and is classified as an anaerobic bacterium; *Staphylococcus aureus* is a systemic pathogen related to infection[33] and is an aerobic bacterium. These selected strains were representative of the oral microecological environment.

3.3.1 Bacterial growth curve. The bacterial growth curves are shown in Fig. 8. As the content of MHD-QAC antibacterial

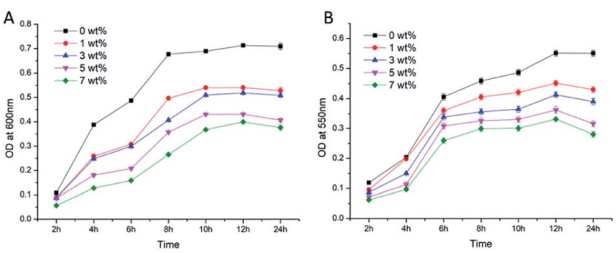

Fig. 8 Bacterial growth curve (A): *S. mutans*; (B): *S. aureus*.

Table 3 Colonies and antibacterial rate of *S. mutans* by the film test (%, $\bar{x} \pm s$)[a]

Group	0 wt%	1 wt%	3 wt%	5 wt%	7 wt%
Colony number	1216 ± 39.6^{a}	85 ± 6.2^{b}	46 ± 3.5^{c}	9 ± 0.8^{d}	7 ± 0.4^{d}
Antibacterial rate	0	93.01	96.22	99.26	99.42

[a] Note: the lower case letters indicated statistical differences within a row ($P < 0.05$).

Table 4 Colonies and antibacterial rate of *S. aureus* by the film test (%, $\bar{x} \pm s$)[a]

Group	0 wt%	1 wt%	3 wt%	5 wt%	7 wt%
Colony number	854 ± 25.3^{a}	72 ± 5.2^{b}	38 ± 2.1^{c}	6 ± 0.5^{d}	5 ± 0.4^{d}
Antibacterial rate	0	91.57	95.56	99.30	99.41

[a] Note: the lower case letters indicated statistical differences within a row ($P < 0.05$).

polymer increased, the OD of the bacterial suspension at the same time point decreased, indicating that the bacterial density decreased as the MHD-QAC antibacterial polymer increased. In addition, the material exhibited concentration-dependent bacterial growth inhibition.

3.3.2 Colony counting by film test. The antibacterial results of the film test were shown in Tables 3 and 4. With the increase of MHD-QAC antibacterial polymer content, the number of bacterial colonies of the two bacteria decreased significantly, in which the 0 wt% group was the most and the 7 wt% group was the least. No significant difference was noted between the 5 wt% group and 7 wt% group ($P > 0.05$). The results of the antibacterial rate showed that the antibacterial rates of the 5 wt% group and 7 wt% group were greater than 99%, belonging to grade I, with a strong antibacterial effect, indicating that the antibacterial group ($-NH^{2+}$) of MHD-QAC was not damaged. The antibacterial rates of the 1 wt% group and 3 wt% group belong to grade II, indicating that they have antibacterial activity.

3.3.3 Bacterial adhesion test. (1) Bacterial adhesion plate colony count

The antibacterial results of the adhesion test were shown in Tables 5 and 6. With the increase of MHD-QAC antibacterial polymer content, the number of bacterial colonies of the two bacteria decreased significantly, in which the 0 wt% group was the most and the 7 wt% group was the least. No significant difference was noted between the 5 wt% and 7 wt% groups ($P > 0.05$). The antibacterial rate results showed that the antibacterial rates of the 5 wt% and 7 wt% groups were greater than 99%, which belonged to grade I. These results indicate that the two groups exhibited strong antibacterial activity. The antibacterial rates of the 1 wt% and 3 wt% groups belong to grade II, showing antibacterial activity. The bacterial adhesion test results demonstrated that a large number of bacteria covered the surface of the 0 wt% group (without the addition of antibacterial agent). With increasing MHD-QAC content, the number of bacteria decreased significantly.

(2) FE-SEM analysis

The FE-SEM results of the bacterial morphology on the surface of the antibacterial epitaxial transition layer specimens are shown in Fig. 9. On the surface of the 0 wt% sample without

Table 5 Colonies and antibacterial rate of *S. mutans* by the adhesion test (%, $\bar{x} \pm s$)[a]

Group	0 wt%	1 wt%	3 wt%	5 wt%	7 wt%
Colony number	1106 ± 30.3^{a}	70 ± 6.8^{b}	37 ± 3.2^{c}	6 ± 0.5^{d}	4 ± 0.3^{d}
Antibacterial rate	0	93.67	96.65	99.46	99.64

[a] Note: the lower case letters indicated statistical differences within a row ($P < 0.05$).

Table 6 Colonies and antibacterial rate of *S. aureus* by the adhesion test (%, $\bar{x} \pm s$)[a]

Group	0 wt%	1 wt%	3 wt%	5 wt%	7 wt%
Colony number	626 ± 30.3^{a}	56 ± 3.2^{b}	22 ± 2.5^{c}	4 ± 0.8^{d}	2 ± 0.2^{d}
Antibacterial rate	0	91.05	96.49	99.36	99.68

[a] Note: the lower case letters indicated statistical differences within a row ($P < 0.05$).

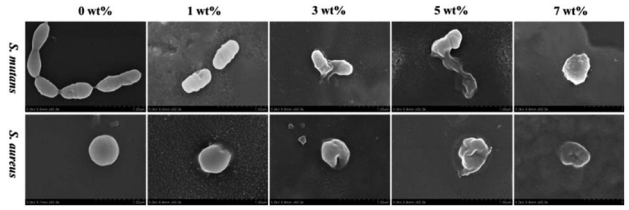

Fig. 9 Bacterial morphology changes as assessed by FE-SEM (×50 000).

MHD-QAC, the bacteria grew well, the bacterial morphology was regular, and the cell wall was complete and smooth. In the 1 wt% group, the bacterial morphology was broken, and the cell wall was rough or incomplete, and slightly concave or even dissolved. Most of the bacteria in the 3 wt%, 5 wt% and 7 wt% groups had serious cell wall damage, cytoplasmic leakage and bacterial dissolution.

3.3.4 Live/dead bacteria fluorescent staining. Fig. 10 shows the BacLight live/dead fluorescent assay of *S. mutans* and *S. aureus* adhered on the zirconia surface. The living bacteria are dyed green, and the bacteria with damaged biofilms are dyed red. When living bacteria and dead bacteria overlap in the same area, they are yellow or orange. The 0 wt% control group of the two bacteria was dyed green, whereas the 1–7 wt% groups with the MHD-QAC antibacterial agent were mostly dyed red. The MHD-QAC had a strong antibacterial effect. As the MHD-QAC content increased, the red area increased, indicating that the number of dead bacteria increased and the bactericidal effect increased.

Based on the above experimental results, the antibacterial epitaxial transition layer has a good bactericidal effect and antibacterial adhesion, and the antibacterial effect of the 5 wt% and 7 wt% groups is significant.

Although the antibacterial mechanism of QACs has not been determined, it is generally believed to be "contact sterilization".[34–38] The antibacterial effect of QACs mainly includes two processes: electrostatic adsorption and membrane destruction. Generally, the surface of bacteria has a negative charge and is stable due to divalent cations such as Mg^{2+} and Ca^{2+}. The negative charge on the surface of Gram-positive bacteria is related to the composition of cell wall acid, polysaccharide and cell membrane, while the lipopolysaccharide and cell membrane of Gram-negative bacteria are the main sources of

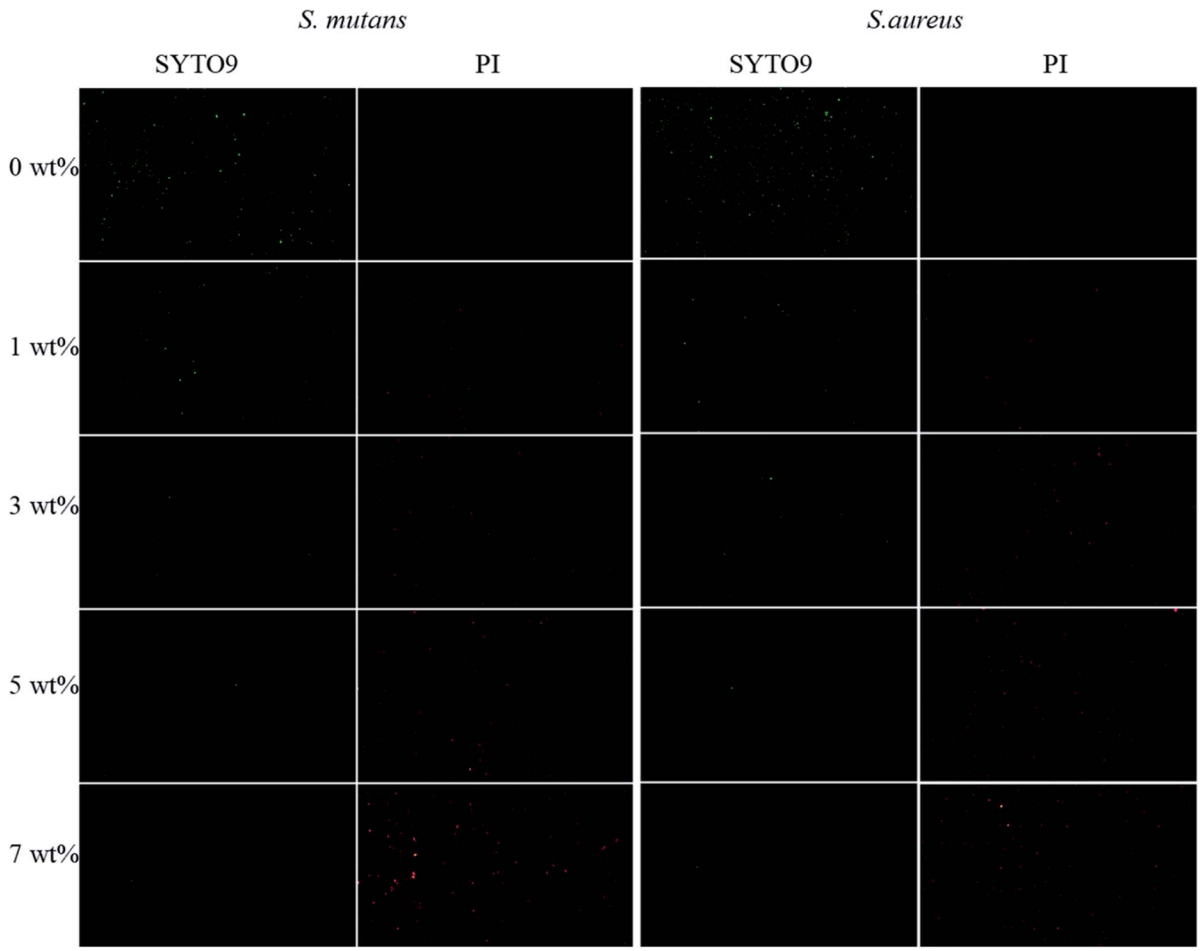

Fig. 10 BacLight live/dead fluorescent assay of *S. mutans* and *S. aureus* adhered on the zirconia surface. Living bacteria are dyed green, dead bacteria are dyed red, and both live and dead bacteria are yellow or orange. Bar = 200 μm.

negative charge.[39] The interaction between macromolecules and Gram-positive bacteria cells may be more effective because their outer layer of polyglycol is fully and loosely packed to promote the polymer chain to penetrate into the cell and interact with the cell plasma membrane. On the other hand, the cells of Gram-negative bacteria have an additional membrane with a bilayer phospholipid structure, which protects the cell plasma membrane to a greater extent from the effect of polymeric biocides.[38] In the structure of the quaternary ammonium salt antibacterial monomer, the hydrophilic head of the quaternary ammonium group with a positive charge can replace the stable Mg^{2+} and Ca^{2+} cations on the bacterial surface, and adsorb on the surface of the negatively charged bacterial cell membrane by electrostatic interaction. Most of the antibacterial activities of quaternary ammonium salts are affected by their surface activity characteristics and hydrophobic chain length.[35–37] The hydrophobic long carbon chain penetrates the cell wall of bacteria by combining with the cell wall components. It interacts with the phospholipid bilayer and membrane protein on the cell membrane, destroys the cell membrane, and causes the enzyme and metabolic intermediate products in the bacteria to overflow. Finally, the respiratory function of the bacteria is inhibited, thereby achieving contact sterilization and bacteriostasis.[40,41]

3.3.5 Shear bond strength. To evaluate the effect of the MHD-QAC antibacterial agent on the bond strength of zirconia ceramics, the SBS of each antibacterial epitaxial transition layer was tested. The SBS of the 0 wt% group is consistent with that in previous work.[26] The SBS results are shown in Table 7. Compared with that of the control group (0 wt%), the SBS of the 1–5 wt% group showed no significant difference ($P > 0.05$), while that of the 7 wt% group decreased ($P < 0.05$), which may be due to the reaction of the hydroxyl group in MHD-QAC with part of the siloxane group in the KH570 hydrolysate, reducing the chemical bonding force between the KH570 hydrolysate and the silicate coating. In addition, the immediate SBS of the 7 wt% group was greater than that of other surface modifications.[42–44] After 5000 thermal cycles, SBS values of all groups exhibited no significant change, showing good durability.

3.3.6 Cytotoxicity *in vitro*. Dental materials are often exposed to the moist environment of the oral cavity, and the penetration of water molecules makes the nonpolymerized components precipitate and become released into the mouth, which may cause potential harm to the human body.[45–47] Therefore, it is necessary to evaluate the biocompatibility of dental materials before their clinical application.

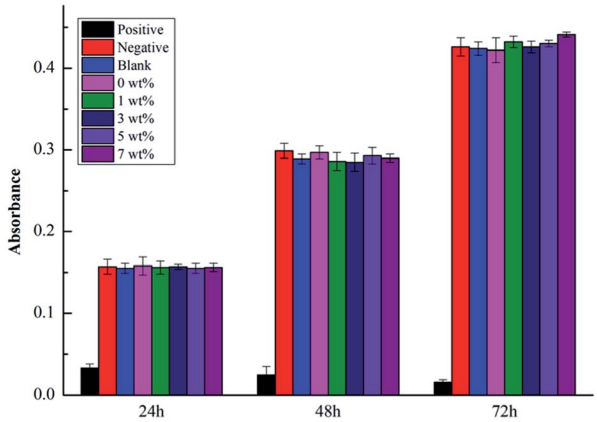

Fig. 11 Absorbance values of L929 cells at different time ($\bar{x} \pm s$).

(1) MTT

The cell absorbance values, RGR values and cytotoxicity grades are shown in Fig. 11 and Table 8. As shown in Fig. 11, at the same time point, the *A* values of the negative control group, blank control group, and experimental groups were basically similar and not significantly different from those of the silicate-based transition film groups ($P > 0.05$). Significant differences were noted between the positive control group and the other groups ($P < 0.01$). As shown in Table 8, at different time points, each experimental group exhibited a good cell relative proliferation rate, which was greater than 90%. The cytotoxicity level was 0 or I, indicating that the material exhibited no obvious cytotoxicity *in vitro*.

(2) Calcein-AM and PI live/dead cell staining

The fluorescent staining results of living/dead cells are shown in Fig. 12. The living cells (green stained) in each experimental group were spindle shaped and well extended. The proportion of living cells in each group was greater than 90%, which was consistent with the results of the MTT toxicity test.

In this study, the MTT toxicity test and calcein-AM and PI live/dead cell staining results showed that the cell survival rate *in vitro* of the antibacterial epitaxial transition layer was greater

Table 7 The SBS of zirconia to resin (MPa, $\bar{x} \pm s$, $n = 9$)[a]

Group	24 hours	5000 cycles
0 wt%	26.38 ± 1.29^{Aa}	26.12 ± 1.52^{Aa}
1 wt%	26.15 ± 0.86^{Aa}	25.81 ± 1.50^{Aa}
3 wt%	25.98 ± 1.57^{Aa}	25.74 ± 1.26^{Aa}
5 wt%	25.63 ± 1.55^{Aa}	25.41 ± 1.46^{Aa}
7 wt%	24.85 ± 0.91^{Ba}	24.63 ± 0.93^{Ba}

[a] Note: the different superscripted letters indicate significant differences within the same column ($P < 0.05$); the different lower case letters indicate significant differences within the same line ($P < 0.05$).

Table 8 RGR and cytotoxicity grade

	RGR (%)			Cytotoxicity grade		
	24 h	48 h	72 h	24 h	48 h	72 h
Positive	21	9	4	IV	IV	IV
Negative	101	103	100	0	0	0
0 wt%	102	103	100	0	0	0
1 wt%	101	99	102	0	I	0
3 wt%	101	99	100	0	I	0
5 wt%	100	101	101	0	0	0
7 wt%	101	100	104	0	0	0

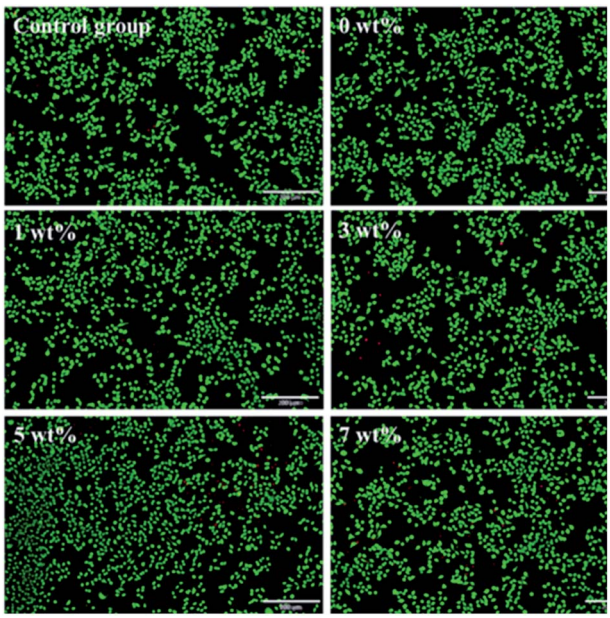

Fig. 12 Fluorescent staining results of living/dead cells. Green cells are living cells, red cells are dead cells. Bar = 200 μm.

than or equal to 99%, which had no effect on L929 cell morphology and proliferation. This result is consistent with previous test results, 26 indicating that the addition of MHD-QAC has no effect on the cytotoxicity of the material.

4 Conclusions

In summary, the antibacterial polymer MHD-QAC was innovatively synthesized by solution polymerization. On the basis of silicate epitaxial transition layer, the antibacterial epitaxial transition layer was successfully prepared by introducing MHD-QAC antibacterial monomer and forming chemical bond with KH570. The antibacterial ingredients are not released and the antibacterial effect is long-lasting. The 5 wt% MHD-QAC antibacterial epitaxial transition layer exhibits a significant antibacterial effects, shear bond strength and cell activity *in vitro*, which can effectively prevent the occurrence of secondary caries. It is of great significance to improve the success rate of clinical zirconia ceramic restorations.

Conflicts of interest

There are no conflicts to declare.

Acknowledgements

This research was financially supported by the National Natural Science Foundation of China (NSFC, Grant No. 81671033) and Ministry of Education's "Chunhui Plan" Cooperative Scientific Research Project. The authors also thank American Journal Experts (AJE) for his assistance in providing language help.

Notes and references

1 A. Hollanders, *Ned. Tijdschr. Tandheelkd*, 2017, **124**, 257–263.
2 I. A. Mjör and F. Toffenetti, *Quintessence Int.*, 2000, **31**, 165–179.
3 J. J. Kruzic, J. A. Arsecularatne, C. B. Tanaka, M. J. Hoffman and P. F. Cesar, *J. Mech. Behav. Biomed. Mater.*, 2018, **88**, 504–533.
4 O. Fejerskov, *Caries Res.*, 2004, **38**, 182–191.
5 L. Cheng, M. D. Weir, K. Zhang, S. M. Xu, Q. Chen, X. Zhou and H. H. K. Xu, *J. Dent. Res.*, 2012, **91**, 460–466.
6 S. Imazato, M. Torii and Y. Tsuchitani, *J. Dent. Res.*, 1993, **30**, 63–68.
7 Y. Zhang, Y. Chen, Y. Hu, F. Huang and Y. H. Xiao, *Dent. Mater. J.*, 2018, **37**, 183–191.
8 H. Zhou, M. D. Weir, J. M. Antonucci, G. E. Schumacher, X. D. Zhou and H. H. K. Xu, *Int. J. Oral Sci.*, 2014, **6**, 77–86.
9 F. Li, M. D. Weir and H. H. K. Xu, *J. Dent. Res.*, 2013, **92**, 932–938.
10 Y. Xue, H. Xiao and Y. Zhang, *Int. J. Mol. Sci.*, 2015, **16**, 3626–3655.
11 S. Imazato, M. Torii, Y. Tsuchitani and J. F. McCabe, *J. Dent. Res.*, 1994, **73**, 1437–1443.
12 C. Zhou, M. D. Weir, K. Zhang, D. M. Deng, L. Cheng and H. H. K. Xu, *Dent. Mater. J.*, 2013, **29**, 859–870.
13 N. Zhang, C. Chen, M. D. Weir, Y. X. Bai and H. H. K. Xu, *J. Dent.*, 2015, **43**, 1529–1538.
14 L. Huang, Y. H. Xiao, X. D. Xing, F. Li, S. Ma, L. L. Qi and J. H. Chen, *Arch. Oral Biol.*, 2011, **56**, 367–373.
15 S. Buffetbataillon, P. Tattevin, M. Bonnauremallet and A. J. Gougeon, *Int. J. Antimicrob. Agents*, 2012, **39**, 381–389.
16 P. Gilbert and L. E. J. Moore, *J. Appl. Microbiol.*, 2010, **99**, 703–715.
17 P. Makvandi, R. Jamaledin, M. Jabbari, N. Nikfarjam and A. Borzacchiello, *Dent. Mater. J.*, 2018, **34**, 851–867.
18 S. Beyth, D. Polak, C. Milgrom, S. Matanis and N. Beyth, *J. Antimicrob. Chemother.*, 2013, **69**, 854–855.
19 C. Susin, M. Qahash, J. Hall, L. Sennerby and U. M. E. Wikesjö, *J. Clin. Periodontol.*, 2008, **35**, 270–275.
20 Y. Yang, L. Huang, Y. Dong, H. C. Zhang, W. Zhou, J. H. Ban, J. J. Wei, Y. Liu, J. Gao and J. H. Chen, *PLoS One*, 2014, **9**, e112549.
21 M. A. Melo, J. Wu, M. D. Weir and H. H. Xu, *J. Dent.*, 2014, **42**, 1193–1201.
22 F. Li, F. Li, D. Wu, S. Ma, J. Gao, Y. Q. Li, Y. H. Xiao and J. H. Chen, *J. Am. Dent. Assoc., JADA*, 2011, **142**, 184–193.
23 N. Hirose, R. Kitagawa, H. Kitagawa, H. Maezono, A. Mine, M. Hayashi and S. Imazato, *J. Dent. Res.*, 2016, **95**, 1487–1493.
24 S. O. Ahmet, M. M. Mutluay, P. Z. Seyfioglu, D. R. Seseogullari, B. Bek and M. A. Tezvergil, *Acta Odontol. Scand.*, 2014, **72**, 831–838.
25 F. M. Korkmaz, T. Tüzüner, O. Baygin, C. K. Buruk, R. Durkan and B. Bagis, *J. Prosthet. Dent.*, 2013, **110**, 107–115.
26 L. Huang, F. Yu, X. Sun, Y. Dong, P. T. Lin, H. H. Yu, Y. H. Xiao, Z. G. Chai, X. D. Xing and J. H. Chen, *Sci. Rep.*, 2016, **6**, 33858.

27 Y. M. Pupo, P. V. Farago, J. M. Nadal, A. C. Kovalik, d. F. A. Santos, O. M. Gomes and J. C. Gomes, *Arch. Oral Biol.*, 2015, **60**, 1138–1145.
28 X. J. Liu, H. Wang, S. Y. Yu, Q. Zhao, Z. S. Shi, Z. C. Cui and S. Zhu, *RSC Adv.*, 2020, **10**, 32476–32484.
29 USP XXII, NF XVII [S], United States Pharmacopeial Convention, Inc, 1990, 2069.
30 X. J. Liu, K. Gan, H. Liu, X. Q. Song, T. J. Chen and C. C. Liu, *Dent. Mater. J.*, 2017, **33**, e348–e360.
31 M. Hotta, H. Nakajima, K. Yamamoto and M. Aono, *J. Oral Rehabil.*, 1998, **25**, 485–489.
32 A. Aamdal-Scheie, W. M. Luan, G. Dahlen and O. Fejerskov, *J. Dent. Res.*, 1996, **75**, 1901–1908.
33 T. Matsuura, Y. Abe, Y. Sato, K. Okamoto, M. Ueshige and Y. Akagawa, *J. Dent.*, 1997, **25**, 373–377.
34 E. R. Kenawy, F. A. Hay, A. E. R. R. E. Shanshoury and M. H. E. Newehy, *J. Polym. Sci., Part A: Polym. Chem.*, 2002, **40**, 2384–2393.
35 S. Imazato, J. H. Chen, S. Ma, N. Izutanic and F. Li, *Jpn. Dent. Sci. Rev.*, 2012, **48**, 115–125.
36 L. Caillier, E. T. Givenchy, R. Levy, Y. Vandenberghe, S. Géribaldi and F. Guittard, *Eur. J. Med. Chem.*, 2009, **44**, 3201–3208.
37 L. Marcotte, J. Barbeau and M. Lafleur, *J. Colloid Interface Sci.*, 2005, **292**, 219–227.
38 A. Muñoz-Bonilla and M. Fernández-García, *Prog. Polym. Sci.*, 2012, **37**, 281–339.
39 K. P. C. Minbiole, M. C. Jennings, L. E. Ator, J. W. Blacka, M. C. Greniera, J. E. LaDow, K. L. Caran, K. Seifert and W. M. Wuest, *Tetrahedron*, 2016, **72**, 3559–3566.
40 B. Ahlström, R. Thompson and L. Edebo, *APMIS*, 1999, **107**, 318–324.
41 N. Kawabata and M. Nishiguchi, *Appl. Environ. Microbiol.*, 1988, **54**, 2532–2535.
42 C. Y. Lung, E. Kukk and J. P. Matinlinna, *Dent. Mater. J.*, 2013, **32**, 165–172.
43 C. Y. Lung, M. G. Botelho, M. Heinonen and J. P. Matinlinna, *Dent. Mater. J.*, 2012, **28**, 863–872.
44 H. Xie, F. R. Tay, F. Zhang, Y. Lu, S. P. Shen and C. Chen, *Dent. Mater. J.*, 2015, **31**, e218–e225.
45 G. A. Arossi, M. Lehmann, R. R. Dihl, M. L. Reguly and H. H. R. Andrade, *Basic Clin. Pharmacol. Toxicol.*, 2010, **106**, 124–129.
46 M. A. P. Borges, I. C. Matos and L. C. Mendes, *Dent. Mater. J.*, 2011, **27**, 244–252.
47 M. Goldberg, *Clin. Oral Investig.*, 2008, **12**, 1–8.